PHYSICAL REVIEW A, VOLUME 61, 020501(R)

Evolution of the germanium $K\beta'''$ x-ray satellites from threshold to saturation

C. Sternemann,[1] A. Kaprolat,[2] M. H. Krisch,[2] and W. Schülke[1]
[1]*Institute of Physics, University of Dortmund, D-44221 Dortmund, Germany*
[2]*European Synchrotron Radiation Facility, F-38043 Grenoble, France*
(Received 31 August 1999; published 18 January 2000)

A study of the photoexited Ge $K\beta'''$ x-ray satellites from onset to saturation using inelastic x-ray scattering is presented. The assignment of the satellites to $[1s3d]$ and $[1s3p]$ excitation channels is confirmed by determination of their different threshold energies and energy positions on the high-energy tail of the $K\beta_2$ fluorescence line. Direct measurement of the variation of the satellite intensities with increasing excitation energy exhibits a long saturation range to the sudden limit and yields indication for the opening of a $[1s3s]$ excitation channel to the $[1s3p]$ satellite. In this work we separate the contributions of the double-electron excitations to the absorption spectrum and show pure satellite spectra for possible application in experiment based extended x-ray-absorption fine-structure background subtraction taking into account the full properties of the solid state.

PACS number(s): 32.30.Rj, 32.70.−n, 32.80.Fb, 61.10.Ht

During ionization and inner-shell excitation a finite probability of the ejection of a second electron into unoccupied bound (shake-up) or continuum states (shake-off) is given due to the change of the central potential by inner-shell vacancy creation [1]. These shake processes cause discontinuities in x-ray absorption [2,3] and satellites in photoemission, inverse photoemission, and fluorescence spectroscopy [4–6]. In the sudden limit, when the electron is ejected immediately and the remaining electrons cannot adapt to the rapid change in potential at high excitation energies, the creation of the core hole and the excitation of the second electron can be treated as two independent ionization processes. On the contrary, for low excitation energies in the adiabatic limit the shake process becomes dependent on the core ionization and provides information about correlation and excitation dynamics [7–9].

The double-excitation phenomena have been widely studied in the sudden limit and are satisfyingly treated from the theoretical side by using the frozen-core approximation, which nevertheless breaks down in the onset regime [7,10,11]. Threshold energies for the shake processes and energy positions of the satellite lines can be well estimated either using the $Z+1$ model [12,13] or within relativistic Dirac-Fock calculations [14]. The variation of the satellite intensity with increasing excitation energy is described for instance by Hartree-Fock calculations [15] or application of the Thomas model [16], which represents the transition from adiabatic to the sudden limit using time-dependent perturbation theory. However, reliable relative satellite intensities and shapes in the near-threshold regime cannot be obtained from these calculations.

The influence of double-excitation processes in x-ray absorption spectroscopy (XAS) is of wide interest [2] and has been studied on several systems [17–21], where small jumps in the atomic background are related to double-electron excitation edges, and resulting artefacts in the Fourier transform of the extended x-ray-absorption fine-structure (EXAFS) signal for small R are traced back to the corresponding background anomalies. Therefore, the consideration of multielectron excitations in the EXAFS data processing scheme is mandatory when the structural signals are weak. Filipponi and Di Cicco [22] successfully applied the GNAXS [23] method in the x-ray absorption spectra of Ge, where $[1s3d]$ and $[1s3p]$ double-excitation contributions are simulated by empirically determined rounded step functions. Furthermore, the Ge $[1s3p]$ double-excitation background was extracted from EXAFS spectra utilizing combined information of different samples of the same element [24], where the structural signal was separated by an *ab initio* XAFS model within the FEFF code.

X-ray emission spectroscopy provides a suitable tool to study double-excitation satellites from onset to saturation without inclusion of model functions into the data evaluation scheme. First detailed photoexcitation measurements were performed by Deslattes *et al.* [6], where both emission and absorption spectroscopy are combined to examine multielectron vacancies on atomic Ar, and more recently by Deutsch and co-workers [14,25] finding a pure shake-off behavior of the Cu $K\alpha$ x-ray satellite complex. Hitherto no measurements of valence fluorescence satellites of a solid have been available. They are of special interest for EXAFS studies since (i) their threshold energies are within the EXAFS regime and (ii) there is no theoretical model to describe the complete satellite evolution.

In this paper we present an x-ray emission study of Ge $K\beta_2$ valence fluorescence satellites from onset in the adiabatic to saturation in the sudden approximation limit. Threshold energies and energy positions are determined and confirm the assignment of the two satellites to $[1s3d]$ and $[1s3p]$ excitation channels when utilizing the $Z+1$ approximation. Furthermore, strong indications for a $[1s3s]$ contribution are found. Pure satellite intensities as a function of excitation energy are presented in a range up to 800 eV above the absorption edge, and the experimental data are confronted with the Thomas model [16].

The measurements were performed at the x-ray inelastic scattering beamline ID28 at the European Synchrotron Radiation Facility using a Rowland spectrometer [26,27] at 90° scattering angle to reduce the background radiation due to Thomson scattering. The sample was a germanium single crystal and the momentum transfer $\vec{q}$ || to the [110] direction. To obtain sufficient count rates and to minimize the

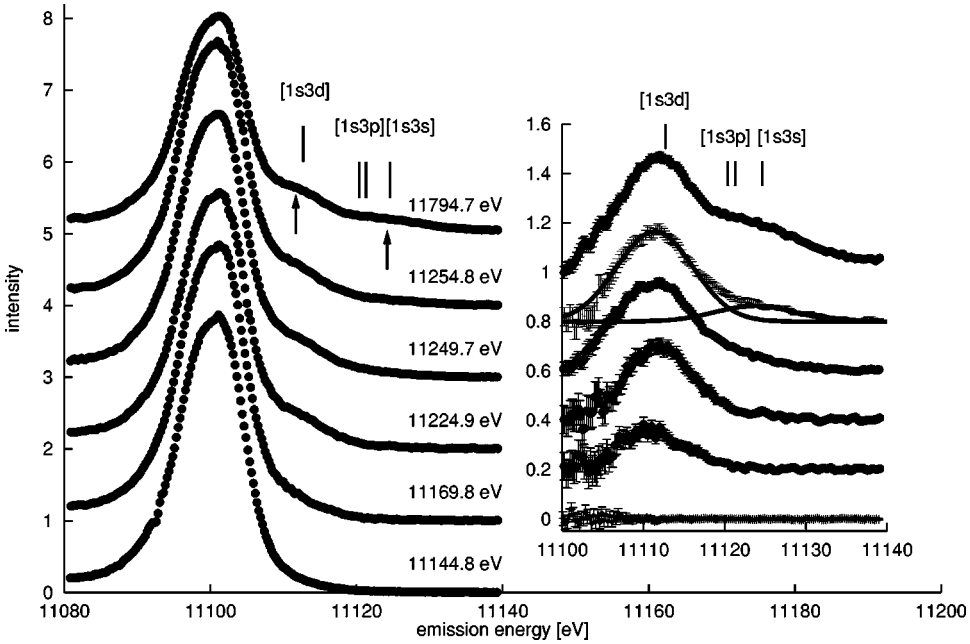

FIG. 1. Evolution of the experimental fluorescence spectra (outscans with points) with increasing excitation energy from the pure fluorescence at 11 144.8 eV to the saturated satellite complex at 11 794.7 eV. The inset shows the double peaked satellite complex after subtraction of the fluorescence contribution. For the spectrum at 11 154.8 eV a Gaussian fit to the two satellites is plotted as a solid line for example. The energy positions of the satellites corresponding to $[1s3d]$, $[1s3p]$, and $[1s3s]$ excitation calculated using the $Z+1$ model are also shown. The arrows indicate the analyzer energies used in the inscans.

influence of the valence-band structure on the emission process [28] the total energy resolution was chosen to be 6.7 eV, so that the absorption process dominated the shape of the spectra. Two different scanning geometries were utilized: first, scanning the analyzer energy from 11 080 to 11 140 eV at fixed incident energies in the range from 11 105 to 11 900 eV (named outscan) to measure the change in shape and the energy positions of the fluorescence line and the satellite complex as a function of incident energy; second, varying the incident energy in the range from 11 060 to 11 800 eV with analyzer energy fixed at the energy positions of the fluorescence and the satellites (named inscan) to get direct access to the threshold energies and the intensity evolution from onset to saturation. Both inscans and outscans were corrected for radiation background and self-absorption in the Ge sample.

Figure 1 shows the evolution of the fluorescence line and the satellite contribution with increasing excitation energy from 11 144.8 to 11 794.7 eV measured in outscan geometry. Subtraction of the pure fluorescence contribution yields the satellite complex, where the fluorescence was determined using outscans measured at excitation energies from 11 135 to 11 145 eV, where the fluorescence shows neither variation in shape due to different influence of the core hole lifetime broadening nor influence of double-ionization processes. The result is presented in the inset of Fig. 1. The satellite spectrum can be separated into two main compounds assigned to $[1s3d]$ and $[1s3p]$, $[1s3s]$ excitation channels, where the $[1s3s]$ satellite is not resolved due to the experimental resolution. To estimate the satellite intensities, widths, and energy positions, both peaks are fitted to Gaussians. As an example, the Gaussian fits of the satellites for the spectrum at 11 254.8 eV are plotted in the inset of Fig. 1 as solid lines. The fit determines the energy position of the $[1s3d]$ satellite to be $11\,111.6\pm1$ eV and of the $[1s3p][1s3s]$ satellite to be $11\,123.6\pm2$ eV below and to $11\,124.8\pm2$ eV above the theoretical threshold energy of the $[1s3s]$ double ionization at 11 307.7 eV. The shift in energy position of the second satellite of 1.2 eV for excitation energies crossing the $[1s3s]$ threshold may indicate the onset of the $[1s3s]$ double excitation. The energy positions are in accordance with the $Z+1$ model results of 11 112.7 eV $(3d)$, 11 120.7 eV $(3p)$, and 11 124.6 eV $(3s)$. In the framework of this model the energy position of the satellite is given by adding the difference between the As and Ge ionization energies for the second ejected electron $(3s,3p,3d)$ to the fluorescence energy. For the $[1s3d]$ and the $[1s3p]$ $[1s3s]$ satellite the saturation intensity in the high-energy range is determined to be $15.7\pm0.9\%$ and $5.5\pm0.5\%$ of the Ge $K\beta_2$ fluorescence intensity. The ratio of the saturation intensities of the two satellites is in good agreement with the calculated ratio using the theoretical excitation probabilities in the sudden limit of Mukoyama and Taniguchi [29].

Furthermore, inscans were performed to achieve high-quality spectra of the satellite evolution from onset to saturation, thus allowing an exact determination of the threshold energies and delivering a better basis for a fit to the Thomas model. The incident energy was scanned from 11 060 to 11 800 eV and the analyzer fixed to 11 111.7 eV (11 124.2 eV) (arrows in Fig. 1) in order to measure the intensity of the $[1s3d]$ ($[1s3p]$,$[1s3s]$) satellite. In addition, the intensity evolution of the fluorescence line was determined by an inscan. To extract the pure satellite intensities the contribution of the fluorescence spectrum underlying the satellite spectra was subtracted by using a scale factor on the fluorescence inscan by which both spectra matched in the energy range from 11 135 to 11 145 eV. For the $[1s3p][1s3s]$ satellite after subtraction of the fluorescence the contribution of the $[1s3d]$ satellite was separated similarly, using the results achieved before. The pure satellite intensities normalized to the fluorescence intensity are plotted in Figs. 2 and 3 as thin solid lines. For comparison, discrete values of the satellite peak intensities obtained from the outscans are plotted with

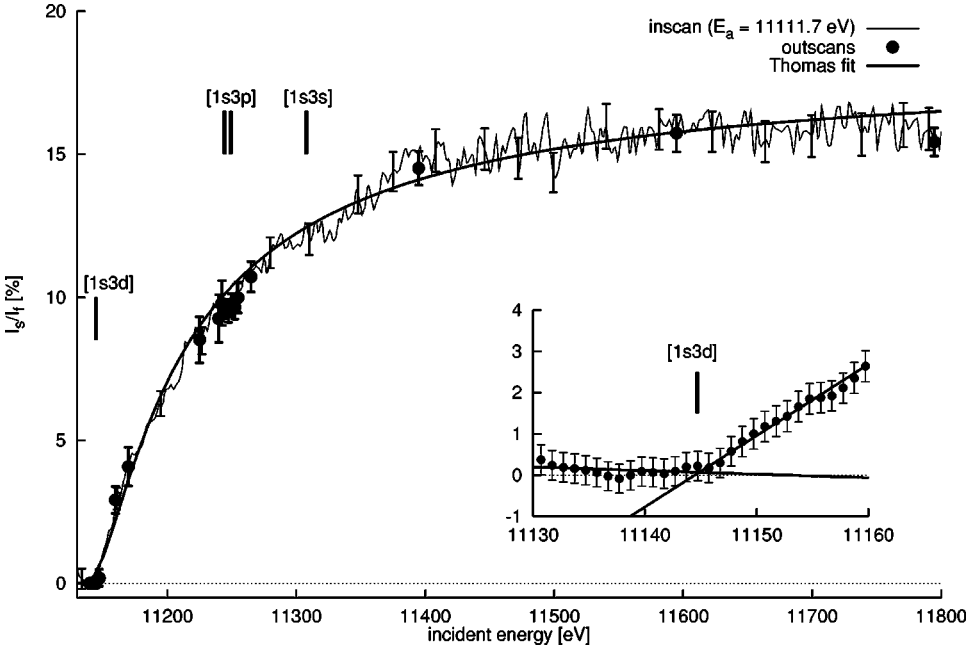

FIG. 2. Intensity evolution of the first satellite measured using inscan geometry with analyzer energy at 11 111.7 eV plotted as a thin solid line with error bars compared to the satellite intensities (points, determined from the outscans, with error bars). The thick solid line shows the fit to the Thomas model of the first satellite. Calculated threshold energies are marked and the threshold regime is magnified in the inset (experimental datapoints) where the intersection of the straight lines determines the experimental threshold energy.

points. The agreement between inscans (thin solid line) and outscans (points) confirms the reliability of the data treatment within the experimental error. The threshold energies were determined from the inscans as shown in the inset of Figs. 2 and 3 by the intersection of two straight lines in the onset regime. For the $[1s3d]$ satellite the threshold energy is determined to be $11\,144.5 \pm 4.0$ eV and $11\,241.6 \pm 4.0$ eV in the case of the $[1s3p]$ double ionization, which is in agreement with the $Z+1$ approximation values of 11 144.7 and 11 245.9 eV. To achieve the threshold energies in the $Z+1$ model the additional energy to excite the second electron is given by the binding energy of the electron in the $Z+1$ system As, assuming a fully screened core hole. Both satellite spectra show a long saturation range up to 550 eV above threshold, which is about 3% of the threshold energy.

The two inscans of the satellites were fitted applying the Thomas model [16], which describes the transition from the adiabatic to the sudden limit of the satellite intensities in a simple mathematical form given by

$$I_{Thomas} = I_\infty \exp\{-r^2 E_s^2/[15.32(E_{ex}-E_{th})]\},$$

where I_∞ is the saturation limit, r is the radius of the shake shell $3d$ $(3p)$, and E_s the shake energy that can be determined using the $Z+1$ model to be 41.7 eV (142.9 eV) according to the ionization energies of As. E_{ex} and E_{th} are the excitation and threshold energies. The adjustable parameters are I_∞, r, and E_{th} in the fit range from 11 130 eV (11235 eV) to 11 800 eV. For the $[1s3d]$ satellite the result of the Thomas fit is plotted in Fig. 2 as a thick solid line. A good agreement in the overall shape is achieved, and the fit

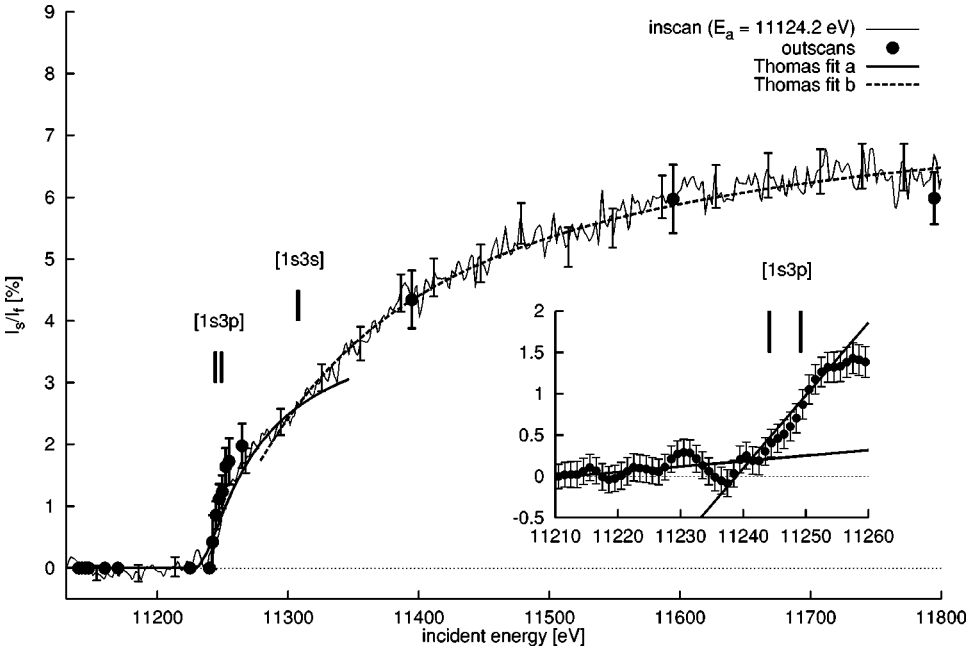

FIG. 3. Same as Fig. 2 but with analyzer energy fixed to 11 124.2 eV, the position of the second satellite. Thomas a and Thomas b denote the different fits to the inscan data according to the separated fit range, showing the two slope regimes due to the opening of the $[1s3s]$ excitation channel.

parameters obtained are $I_\infty = 18.3\%$, $r = 0.784$ Å, and $E_{th} = 11126.8$ eV. The threshold energy is in sufficient agreement with the experimental and theoretical values, but the saturation intensity is wrong due to the inability of the Thomas model to reproduce the correct saturation behavior. On the other hand, the agreement between the Thomas fit and the second satellite in overall shape is poor, especially in the onset regime from 11 240 to 11 340 eV. This agreement in shape is well improved if two independent fits are performed by dividing the fit range into two parts from 11 130 to 11 320 eV (denoted Thomas a) and from 11 290 to 11 800 eV (denoted Thomas b), as shown in Fig. 3. Therefore, the inscan of the $[1s3p][1s3s]$ satellite shows two different slope regimes: (i) from 11 241.6 to 11 305.0 eV, where the upper limit is given by the intersection of the two fitted lines and (ii) from 11 305.0 eV to the saturation limit. The threshold energy of $11\,305.0 \pm 30.0$ eV agrees very well with the theoretical threshold energy for the $[1s3s]$ double excitation of 11 307.7 eV. Thus a strong indication for the opening of the $[1s3s]$ excitation channel at 11 305 eV is given, and hence the application of the Thomas model cannot deliver reliable results due to the mixing of the $[1s3p]$ and $[1s3s]$ contributions in the second inscan. Nevertheless, the fits to the Thomas model for both satellites $[1s3d]$ and $[1s3p][1s3s]$ show deviations from the experiment in the onset regime, which could be assigned to solid-state effects.

In conclusion, this study presents an alternative measurement of the germanium valence fluorescence double excitation satellites from onset to the saturation limit. The assignment of the satellites to $[1s3d]$ and $[1s3p]$ double-excitation edges is confirmed by determination of the energy positions and threshold energies. Furthermore, strong indications for the contribution of the $[1s3s]$ excitation channel to the $[1s3p]$ satellite are found. Two different scanning geometries were used providing the same experimental results and confirming the reliability of the data evaluation procedure. Application of the Thomas model to the experiment failed in the onset regime and overestimated the saturation intensity, but gave good agreement in the intermediate energy range. The high-quality valence satellite spectra as obtained in this study provide a method for determining EXAFS double-excitation background directly by an experiment. This method should find application in the case of highly disordered solids and liquids, where the consideration of the double-ionization features in the background is necessary due to the low structural signals.

This work was supported by the German Federal Ministry of Education Research under Contract No. 05 ST 8 HRA. One of us (A.K.) is indebted to the Deutsche Forschungsgemeinschaft for financial support. We acknowledge the work of D. Gambetti, B. Gorges, M. Lorenzen, K. Martel, and J. F. Ribois during the construction and the commissioning of ID 28. F. Sette is thanked for his encouragement in this project.

[1] T. Åberg, in *Proceedings of the International Conference on Inner-Shell Ionization Phenomena and Future Applications*, edited by R. W. Fink, S. T. Manson, J. M. Palms, and P. Venugopala Rao, U. S. AEC Report No. CONF-720404 (National Technical Information Service, U. S. Dept. of Commerce, Springfield, VA, 1972), p. 1509

[2] A. Filipponi, Physica B **208&209**, 29 (1995).

[3] A. Kodre, S. J. Schaphorst, and B. Crasemann, in *X-Ray and Inner-Shell Processes*, edited by T. A. Carlson, M. O. Krause, and S. T. Manson (AIP, New York, 1990), and references therein.

[4] K. Siegbahn, C. Nordling, G. Johansson, J. Hedman, P. F. Hedén, K. Harmin, U. Gelius, T. Bergmark, L. O. Werme, and Y. Bear, *ESCA Applied to Free Molecules* (North-Holland, Amsterdam, 1969).

[5] T. Mukoyama and Y. Ito, Nucl. Instrum. Methods Phys. Res. B **87**, 26 (1994).

[6] R. D. Deslattes, R. E. La Villa, P. L. Cowan, and A. Henins, Phys. Rev. A **27**, 923 (1983).

[7] B. Crasemann, J. Phys. (Paris) Colloq. **48**, C9-389 (1987).

[8] M. O. Krause and C. D. Caldwell, Phys. Rev. Lett. **59**, 2736 (1987).

[9] J. Tulkki, Phys. Rev. Lett. **62**, 2817 (1989).

[10] *Atomic Inner-Shell Physics*, edited by B. Crasemann (Plenum, New York, 1986).

[11] V. Schmidt, Rep. Prog. Phys. **55**, 1483 (1992).

[12] M. J. Druyvesteyn, Z. Phys. **48**, 707 (1927).

[13] M. Deutsch, Phys. Rev. A **39**, 3956 (1989), and references therein.

[14] M. Fritsch, C. C. Kao, K. Hämäläinen, O. Gang, E. Förster, and M. Deutsch, Phys. Rev. A **57**, 1686 (1998).

[15] S. J. Schaphorst, A. F. Kodre, J. Ruscheinski, B. Crasemann, T. Åberg, J. Tulkki, M. H. Chen, Y. Azuma, and G. S. Brown, Phys. Rev. A **47**, 1953 (1993).

[16] T. D. Thomas, Phys. Rev. Lett. **52**, 417 (1984).

[17] S. I. Salem, Brahm Dev, and P. L. Lee, Phys. Rev. A **22**, 2679 (1980).

[18] G. Li, F. Bridges, and G. S. Brown, Phys. Rev. Lett. **68**, 1609 (1992), and references therein.

[19] A. Filipponi, T. A. Tyson, K. O. Hodgson, and S. Mobilio, Phys. Rev. A **48**, 1328 (1993).

[20] J. Chaboy, A. Marcelli, and T. A. Tyson, Phys. Rev. B **49**, 11 652 (1994).

[21] A. Filipponi and A. Di Cicco, Phys. Rev. A **52**, 1072 (1995).

[22] A. Filipponi and A. Di Cicco, Phys. Rev. B **51**, 12 322 (1995).

[23] A. Filipponi, A. Di Cicco, T. A. Tyson, and C. R. Natoli, Solid State Commun. **78**, 265 (1991).

[24] J. Padežnink Gomilšek, A. Kodre, I. Arčon, A. M. Loireau-Lozac'h, and S. Bénazeth, Phys. Rev. A **59**, 3078 (1999).

[25] M. Deutsch, O. Gang, K. Hämäläinen, and C. C. Kao, Phys. Rev. Lett. **76**, 2424 (1996).

[26] W. Schülke, A. Kaprolat, Th. Fischer, K. Höppner, and F. Wohlert, Rev. Sci. Instrum. **66**, 2446 (1995).

[27] C. C. Kao, W. A. Caliebe, J. B. Hastings, K. Hämäläinen, and M. H. Krisch, Rev. Sci. Instrum. **67**, 1 (1996).

[28] H. Enkisch, A. Kaprolat, W. Schülke, M. H. Krisch, and M. Lorenzen, Phys. Rev. B **60**, 8624 (1999).

[29] T. Mukoyama and K. Taniguchi, Phys. Rev. A **36**, 693 (1987).